Raman Spectroscopy and Microscopy: Solving Outstanding Problems in the Life Sciences

This first article in a two-part series will examine Raman spectroscopy applications in tumor surgery, endoscopy, bacterial identification and more. The second part will cover applications in cell sorting, laser trapping and probing biology.

BY DR. MARINELLA G. SANDROS, UNIVERSITY OF NORTH CAROLINA AT GREENSBORO, AND DR. FRAN ADAR, HORIBA SCIENTIFIC

Raman spectroscopy has become a mature analytical tool, as evidenced by its presentation at the Waters Symposium at the Pittsburgh Conference in 2003 and the subsequent explosion of publications and presentations in the analytical sciences. This is a result of simplification, increased sensitivity and automation of the equipment over the past 20 to 30 years. In addition, the availability of multiple laser wavelengths whose choice is tailored to a particular application, as well as mature spectroscopic software, including multivariate algorithms coupled to two- and three-dimensional imaging, enhance the application of the technology.

This article will cover the areas where Raman has made some impressive gains in the biomedical sciences. These will include imaging to define tumor margins not apparent from standard histology, continued development of miniaturized probes for endoscopic applications, identification of bacteria at the species and strain level, surface-enhanced Raman spectroscopy for signal enhancement targeted to specific analytes, and coupling to atomic force microscopy systems, enabling tip-enhanced Raman spectroscopy for nanoscale resolution.

Identifying tumor margins

The gold standard for tumor margin identification ex vivo has been the hematoxylin and eosin (H&E) staining on fixed or frozen tissue sections. For in vivo analysis, identification of tumor margins during surgery using bright-field microscopy is limited. For example, the challenge is to excise a brain tumor without removing healthy tissue or leaving remnants of the tumor behind. However, these shortcomings can be circumvented by using label-free Raman microscopy, where the molecular composition of a tissue can be nondestructively characterized in real time.

Spontaneous Raman microscopy has been used to analyze the chemical fingerprint of biological specimens such as tissue,[1,2] bones[3,4] and bacteria.[5,6] However, to assess vital tissue, the acquisition speed of spontaneous Raman is slow.[7] Stimulated Raman scattering (SRS)[8] microscopy provides fast image acquisition, as does coherent anti-Stokes Raman spectroscopy (CARS)[8,9] because of the stimulated and coherent nature of these processes. Both techniques offer higher signal intensity than SRS, as well as 3-D spatial resolution.

Defining tumor margins is especially important during the removal of brain tumors. Fast imaging of unstained cryosectioned mouse brain tissue was successfully analyzed with CARS[10] by providing high spectral resolution of tumor infiltration and chemical identification. As shown in Figure 1 (a-d), healthy tissue (high-lipid region) appeared brighter than cancerous tissue because tumor progression modifies the structure and molecular composition (low lipid). The study concluded that tumor margins were easily discerned down to a few cells and were complementary with H&E staining (Figure 1, e-h). In addition, CARS was used for live-brain imaging of myelin fiber,[11] but image and data processing is cumbersome because the nonresonating background distorts the signals. Conse-

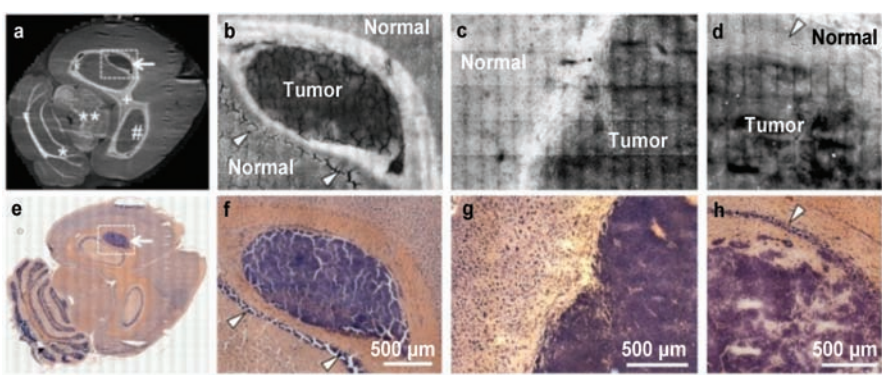

Figure 1. CARS image of **(a)** a whole mouse brain where the white arrow indicates the localization of human glioblastoma, **(b)** a magnified image of the dashed rectangle in **a**, **(c)** breast cancer metastasis and **(d)** metastasis of melanoma. CARS images represent a linear combination of symmetric C-H groups at 2850 cm^{-1} and 2930 cm^{-1}. **(e-f)** H&E stainings of consecutive sections corresponding to **a-d**. Nuclei-rich layers in gray matter are specified by the white arrow. Adapted with permission from Uckermann et al.[10]

quently, CARS might not be appropriate for a surgical setting.

In comparison to CARS,[12,13] SRS microscopy has a greater potential to be integrated into surgical suites[14] because there is no nonresonant background. It is directly comparable to spontaneous Raman with a concentration-dependent signal. Recently, Ji et al[15] took advantage of these unique properties of SRS microscopy, demonstrating its use for the real-time identification of tumor margins in mice brain tissue (in vivo) where boundaries were not directly visible. Under bright-field microscopy (Figure 2), the brain tissue of a mouse 24 days after implantation with a human glioblastoma multiforme (GBM) xenograft appears normal. However, with SRS microscopy, tumor tissue was delineated easily by the higher nuclear-to-cytoplasmic ratio. Furthermore, tissue taken from a human patient with GBM was analyzed ex vivo, and a direct correlation was observed between SRS microscopy and H&E staining in detecting tumor margins.[15]

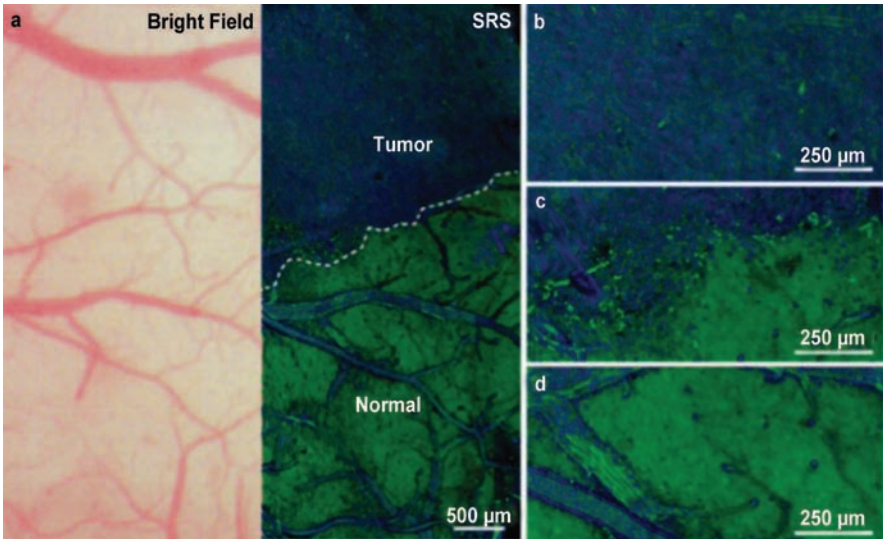

Figure 2. (a) Comparison of a bright-field microscopy image of a mouse brain with stimulated Raman scattering (SRS) microscopy; dashed line indicates the tumor margin. **(b-d)** High-magnification SRS images within the tumor **(b)**, at the tumor-brain interface **(c)** and within normal brain **(d)**. SRS images represent a linear combination of symmetric stretching of C-H Raman signals at 2845 and 2930 cm^{-1}. Adapted with permission from Ji et al.[15] Copyright 2013 Clearance Center.

Catheters and endoscopic probes

An important goal for the medical community is to enable Raman measurements through an endoscope in the operating room theater or outpatient setting. Extensive study of atherosclerosis, cancer and bone disease indicates that in situ Raman measurements will have an enormous impact. A variety of remote Raman probes have been designed over the past 25 years.

Significant hurdles to be overcome include filtering the silica Raman signal generated in the laser delivery fiber and the laser signal reflected back to the collection fibers. For endoscopic applications, it was proposed that one fiber would deliver the laser while a bundle of fibers, usually arranged concentrically around the laser fiber, would collect the Raman signals. In such devices, the silica signal in the laser delivery fiber is blocked by a laser bandpass filter mounted directly on the fiber tip. In addition, the reflected laser light from the sample is blocked by long-pass filter(s) mounted directly on the collection fibers. This solution tends to be bulky and labor-intensive to produce; therefore, it is expensive and not reusable for multiple patients.

Recently, Dochow et al[16] designed and produced multicore fibers containing fiber Bragg gratings[17] that effectively transmit the Raman signal while filtering the strong Rayleigh signal at the laser wavelength. Their design included 19 single-mode cores in a multicore single-mode fiber that optimized collection efficiency. A Raman probe was constructed by bundling six such fibers around a laser-excitation fiber in a 1.5-mm OD steel capillary and fixing the fibers with cyanoacrylate adhesive. (It is believed that the dimension can be further reduced to ~375 µm.) At the spectrograph end, the six collection fibers were arranged in a line to match the entrance slit and to further optimize detection of the Raman light. Raman tests indicated the presence of silica signal, but it was determined that it was generated in the laser delivery fiber, which at that point had not been filtered.

Another interesting innovation in fiber probes for Raman is the use of a ball lens at the probe tip; this lens serves both to focus the laser and to collect the Raman light, eliminating much focusing irreproducibility.[18-20] Such a lens was implemented in 2004 to quantify fat and carotenoids in Atlantic salmon.[21] In the same year, it was used in a probe consisting of an illumination fiber surrounded by collection fibers in a tube measuring only 2 mm in diameter.[22] In 2008, a ball lens with a hollow fiber was used for in vivo subsurface analysis of biomedical tissue.[23]

Once commercialized and combined with adequate databases and discrimination algorithms, these probes will enable Raman measurements to be implemented in the clinical setting.

Rapid bacterial identification

It has become clear within the past 10 years that it is possible not only to record spectra of individual bacteria, but also to identify them at the species level and to differentiate them at the strain level. This has important implications at the point of care, because currently it takes several days to culture and identify pathologic organisms and to choose an effective antibiotic therapy. In the interim, broad-spectrum antibiotics are used to protect the patient, but these can produce antibiotic-resistant strains of the pathogen.

To implement Raman identification of bacteria, it is important to recognize that a genetically homogeneous cell population can be phenotypically heterogeneous for a variety of environmental conditions that can up- or down-modulate gene expression; this in turn will affect the relative contributions of the proteins, lipids, carbohydrates and nucleic acids in the Raman spectrum. Consequently, the sorting algorithm and database assembled to make identifications must take these variations into account.

Although Raman spectra of bacterial populations had been measured before 2000, in that year the first report appeared of measurements of single bacterial cells.[24] While this work was motivated more from the point of view

It has become clear within the past 10 years that it is possible not only to record spectra of individual bacteria, but also to identify them at the species level and to differentiate them at the strain level.

of biotechnology (the organism studied, *Clostridium beijerinckii*, is an anaerobic biocatalyst), the authors showed that the molecular compositions of morphologically differentiated cells were different. In particular, in a 47-hour culture that had already shifted to solvent production (butanol, acetone, butyrate and acetate), enlarged cells were observed, and the Raman spectrum showed accumulation of storage polysaccharide granulose (peak at 481 cm^{-1}).

In 2002, Maquelin et al[25] reviewed the literature showing that bacterial and yeast species and strains could be discriminated by Fourier transform IR and Raman spectroscopies. Most of the work described in this article was not done on individual organisms, but the advantages of microsampling were explored. Most importantly, the use of multivariate techniques for extracting the relevant information was described.

In 2003, Rösch et al[26] reported spectra of monolayers of bacterial smears and single bacteria. For colored species, the spectra were dominated by the resonance-enhanced carotenoids that provided differentiation of species.

In 2004, Huang and his colleagues[27] also showed that, in combination with multivariate algorithms, it is possible to differentiate bacteria of distinct species, presumably based on varying abundances of the molecular components. In addition, they importantly showed that growth phases of a particular species could be differentiated. Finally, they showed that, by isotopic substitution, they could follow uptake of specific substrates (e.g., glucose) by tracking mass-dependent peak shifts in the vibrational spectrum.

In 2009, Hermelink et al[28] reported success in documenting heterogeneity in microbial populations by recording spectra of single bacterial cells. They studied three types of bacteria that, in response to environmental triggers, produce molecular entities other than proteins, lipids, carbohydrates and nucleic acids. Images of *Bacillus thuringiensis* acquired during the stationary growth stage showed the presence of Ca^{2+}-dipicolinic acid in the endospore, as well as the Bt toxin, a protein produced for its ability to kill insects. Images of dry *Legionella bozemanii* show the presence of poly-β-hydroxybutyric acid (PHB), a product for energy storage that appears after physiological stress. Images of *Bacillus cereus* show three components: PHB, picolinate in the spores, and protein.

In 2009, Harz et al[29] wrote a review on the use of Raman (and IR) microscopy for identifying both bacteria and yeast cells. They pointed out that not only is it important to develop rapid identification of bacteria at the strain level for clinical applications, but microbial identification is also important for food quality control and pharmaceutical/cosmetic manufacturing. They were careful to note that bacteria can be qualified by single spectra because the size of the bacterium is commensurate with the laser focus; however, characterization of yeast cells requires mapping to capture all of the spectral information in the organism whose size is of the order of 10 µm. These authors showed spectra of *E. coli* recorded at different temperatures and nutritional conditions, and of *S. epidermidis* recorded at different ages after the start of culture. Consistent with findings by other authors, these spectra exhibited subtle differences. They cited the work of Neugebauer et al,[30] where the effects of antibiotics on bacteria were documented, and the work of De Gelder et al,[31] who applied two-dimensional spectroscopy (using the time of growth as the variable) to identify which spectral changes correlated with growth.

In 2013, Neugebauer et al[32] studied infectious organisms involved in urinary tract infections, one of the most prevalent disorders in the world. Not only did they report the ability to differentiate species using the support vector machine algorithm, but they also devised a method to study bacteria in the aqueous phase as a means to determine antibiotic sensitivity. Their method is based on dielectrophoresis, which captures multiple bacteria from solution. A more common means for bacterial manipulation is optical trapping, which will be treated in the second article in this two-part series.

Meet the authors

Dr. Marinella G. Sandros is an assistant professor in the Department of Nanoscience at the University of North Carolina at Greensboro; email: m_sandro@uncg.edu. Dr. Fran Adar is the principal Raman applications scientist at Horiba Scientific in Edison, N.J.; email: fran.adar@horiba.com.

References

1. A. Whitley and F. Adar (2006). Confocal spectral imaging in tissue with contrast provided by Raman vibrational signatures. *Cytometry Part A*, Vol. 69A, pp. 880-887.
2. M. Ashtikar et al (2013). Noninvasive depth profile imaging of the stratum corneum using confocal Raman microscopy: First insights into the method. *Eur J Pharm Sci*, Vol. 50, pp. 601-608.
3. S.R. Goodyear (2009). A comparison of cortical and trabecular bone from C57 Black 6 mice using Raman spectroscopy. *Bone*, Vol. 44, pp. 899-907.
4. O. Akkus et al (2003). Aging of microstructural compartments in human compact bone. *Bone and Miner Res*, Vol. 18, pp. 1012-1019.
5. S.H.K. Eder (2014). Submicrometer-scale mapping of magnetite crystals and sulfur globules in magnetotactic bacteria using confocal Raman microspectrometry. *PLOS ONE*, Vol. 9, e107356.
6. R.N. Masyuko (2014). Spatial organization of *Pseudomonas aeruginosa* biofilms probed by combined matrix-assisted laser desorption ionization mass spectrometry and confocal Raman microscopy. *Analyst*, Vol. 139, pp. 5700-5708.
7. H. Yamakoshi (2012). Alkyne-tag Raman imaging for visualization of mobile small molecules in live cells. *J Am Chem Soc*, Vol. 134, pp. 20681-20689.
8. R. Boyd (2008). *Nonlinear Optics*. 3rd ed. Elsevier.
9. M. Bonn et al (2009). Imaging of chemical and physical state of individual cellular lipid droplets using multiplex CARS microscopy. *J Raman Spectrosc*, Vol. 40, pp. 763-769.
10. O. Uckermann et al (2014). Label-free delineation of brain tumors by coherent anti-Stokes Raman scattering microscopy in an orthotopic mouse model and human glioblastoma. *PLOS ONE*, Vol. 9, e107115.
11. Y. Fu et al (2008). Ex vivo and in vivo imaging of myelin fibers in mouse brain by coherent anti-Stokes Raman scattering microscopy. *Opt Express*, Vol. 16, pp. 19396-19409.

12. Y. Ozeki et al (2009). Analysis and experimental assessment of the sensitivity of stimulated Raman scattering microscopy. *Opt Express*, Vol. 17, pp. 3651-3658.
13. C.W. Freudiger et al (2008). Label-free biomedical imaging with high sensitivity by stimulated Raman scattering microscopy. *Science*, Vol. 322, pp. 1857-1861.
14. J.N. Bentley et al (2014). Real-time image guidance for brain tumor surgery through stimulated Raman scattering microscopy. *Expert Rev Anticancer Ther*, Vol. 14, pp. 359-361.
15. M. Ji et al (2013). Rapid, label-free detection of brain tumors with stimulated Raman scattering microscopy. *Sci Transl Med*, Vol. 5, p. 201ra119.
16. S. Dochow et al (2012). Multicore fiber with integrated fiber Bragg gratings for background-free Raman sensing. *Opt Express*, Vol. 20, pp. 20156-20169.
17. R. Kashyap (2010). *Fiber Bragg Gratings*. Academic Press.
18. B.J. Marquardt et al (2001). Demonstration of a high-precision optical probe for effective sampling of solids by Raman spectroscopy. *Proc SPIE*, Vol. 4469, Raman Spectroscopy and Light-scattering Technologies in Materials Science (Oct. 21).
19. B. Marquardt and L. Burgess (2004). Optical Immersion Probe Incorporating a Spherical Lens. U.S. Patent No. 6,831,745 B2.
20. B. Marquardt and L.W. Burgess (2005). Optical Immersion Probe Incorporating a Spherical Lens. U.S. Patent No. 6,977,729 B2.
21. J.P. Wold et al (2004). Rapid quantification of carotenoids and fat in Atlantic salmon (*Salmo salar L.*) by Raman spectroscopy and chemometrics. *Appl Spectrosc*, Vol. 58, pp. 395-403.
22. J. Motz et al (2004). Optical fiber probe for biomedical Raman spectroscopy. *Appl Opt*, Vol. 43, pp. 542-554.
23. Y.S. Yamamoto (2008). Subsurface sensing of biomedical tissues using a miniaturized Raman probe: Study of thin-layered model samples. *Anal Chim Acta*, Vol. 619, pp. 8-13.
24. K.C. Schuster et al (2000). Multidimensional information on the chemical composition of single bacterial cells by confocal Raman microspectroscopy. *Anal Chem*, Vol. 72, pp. 5529-5534.
25. K. Maquelin et al (2002). Identification of medically relevant microorganisms by vibrational spectroscopy. *J Microbiol Methods*, Vol. 51, pp. 255-271.
26. P. Rösch et al (2003). The identification of microorganisms by micro-Raman spectroscopy. *J Mol Struc*, Vols. 661-662, pp. 363-369.
27. W.E. Huang et al (2004). Raman microscopic analysis of single microbial cells. *Anal Chem*, Vol. 76, pp. 4452-4458.
28. A. Hermelink et al (2009). Phenotypic heterogeneity within microbial populations at the single-cell level investigated by confocal Raman microspectroscopy. *Analyst*, Vol. 134, pp. 1149-1153.
29. M. Harz et al (2009). Vibrational spectroscopy – a powerful tool for the rapid identification of microbial cells at the single-cell level. *Cytometry Part A*, Vol. 75A, pp. 104-113.
30. U. Neugebauer et al (2007). The influence of fluoroquinolone drugs on the bacterial growth of *S. epidermidis* utilizing the unique potential of vibrational spectroscopy. *J Phys Chem A*, Vol. 111, pp. 2898-2906.
31. J. De Gelder et al (2007). Methods for extracting biochemical information from bacterial Raman spectra: Focus on a group of structurally similar biomolecules – fatty acids. *Anal Chim Acta*, Vol. 603, pp. 167-175.
32. U. Neugebauer et al (2013). Fast and selective against bacteria. *Opt Photonik*, Vol. 8, pp. 36-39.